



Studies on the conversion of glycerol to 1,2-propanediol over Ru-based catalyst under mild conditions

Seung-Hwan Lee^a, Dong Ju Moon^{a,b,c,*}

^a Clean Energy Research Center, Korea Institute of Science and Technology (KIST), Seoul, Republic of Korea

^b Clean Energy & Chemical Engineering, UST, Republic of Korea

^c Green School, Korea University, Seoul, Republic of Korea

ARTICLE INFO

Article history:

Received 27 October 2010

Received in revised form 15 March 2011

Accepted 26 March 2011

Available online 25 May 2011

Keywords:

1,2-Propanediol (PDO)

Glycerol

Ru

Hydrogenolysis

Hydrotalcite

ABSTRACT

The effects of support in Ru-supported catalyst on the conversion of glycerol and selectivity of 1,2-propanediol (1,2-PDO) were investigated in the hydrogenolysis of glycerol. The Ru-based catalysts were prepared by solid phase crystallization and impregnation methods in order to improve 1,2-PDO selectivity. The prepared catalysts were characterized by N₂ physisorption, CO chemisorption, XRD, TPR, NH₃-TPD and TEM techniques. The catalytic hydrogenation of glycerol was investigated at 453 K, initial H₂ pressure of 2.5 MPa and 20 wt% glycerol aqueous solution for 18 h. It was found that the 5 wt% Ru–CaZnMg/Al catalyst prepared by the solid phase crystallization and impregnation methods showed higher catalytic performance than the other catalysts. The glycerol conversion and 1,2-PDO selectivity obtained were 50% and 85%, respectively. It was found that the selectivity of 1,2-PDO increased with the acidity of catalyst.

© 2011 Published by Elsevier B.V.

1. Introduction

Catalytic conversion of renewable biomass resources, as feedstocks for the chemical industry, becomes more and more important as serious energy and environmental problems are highlighted [1]. Glycerol is a main by-product of biodiesel production derived from biomass such as vegetable oil and palm oil. The recent rapid development of biodiesel processes has caused much concern over the oversupply of glycerol [2]. Excessive production of glycerol from biodiesel production could not only flood the current market for glycerol but also negatively impact the economical aspect of biodiesel. Finding novel processes for converting glycerol to high value-added products can contribute to the economic of the production of biodiesel [2–6]. One of the most attractive approaches of converting glycerol is to produce 1,2-propanediol (1,2-PDO).

It has been reported that 1,2-PDO can be produced through the catalytic conversion of polyols or glycerol [2]. The conversion of glycerol to 1,2-PDO has been carried out at 15 MPa and 513–543 K over Cu- and Zn-based catalysts promoted by sulfided Ru catalyst [7]. The hydrogenolysis of glycerol over the catalyst containing Co, Cu, Mn and Mo and some inorganic polyacid was investigated at

25 MPa and 523 K [8]. The hydrogenolysis reaction over homogeneous catalysts containing W and group VIII transition metals were studied at 32 MPa and 473 K [9].

Recently, hydrogenolysis of glycerol over Cu-based catalysts such as Raney Cu, Cu/C, and Cu–Pt and Cu–Ru bimetallic catalysts were investigated in mild conditions under the reaction pressure of less than 5 MPa and temperature of less than 473 K [10–13]. Dasari et al. reported that 54.8% of glycerol conversion and 85.0% of 1,2-PDO selectivity were achieved on a copper–chromite catalyst at 473 K and 1.4 MPa [14]. Guo et al. reported that 49.6% of glycerol conversion and 96.0% of 1,2-PDO selectivity were achieved on a Cu/γ-Al₂O₃ catalyst at 493 K and 1.5 MPa [15]. These researches about hydrogenolysis of glycerol in mild conditions showed good 1,2-PDO selectivity. However it was reported that the glycerol conversion over Cu-based catalysts was lower than Ru-based catalysts in hydrogenolysis of glycerol in spite of high selectivity of 1,2-PDO [10,11].

Hydrogenolysis reactions of glycerol over activated carbon or alumina supported Ru catalysts combined with various solid acid catalysts such as zeolites, sulfated zirconia, rhenium, niobium and an ion exchange resin were studied at reaction pressure over 8 MPa [16–21]. Generally, it was also reported that the combination of Ru-based catalyst and solid acid catalyst exhibited high catalytic activity and 1,2-PDO selectivity in high pressure over 8 MPa and 393–473 K of temperature. However the degradation of glycerol and the production of ethylene glycol occurred drastically as side reactions in the glycerol hydrogenolysis over the Ru-base catalyst

* Corresponding author at: Clean Energy Research Center, Korea Institute of Science and Technology (KIST), 39-1 Hawolgok-dong, Sungbuk-gu, Seoul, 136-791, Republic of Korea. Tel.: +82 2 958 5867; fax: +82 2 958 5809.

E-mail address: djmoon@kist.re.kr (D.J. Moon).

without modification of solid acid [2,10,22]. However, it has not been reported that hydrogenolysis of glycerol over Ru-based catalyst in the mild conditions.

In this work, the novel types of Ru-based catalysts prepared by solid phase crystallization and impregnation methods without solid acid catalyst were investigated in the hydrogenolysis of glycerol under the mild conditions.

2. Experimental

2.1. Catalyst preparation

The hydrotalcite-like catalysts were prepared by a solid phase crystallization method with some modification [21,23–28]. First, an aqueous ammonium carbonate solution was added to a nitrate solution of Mg and Al. A pH of the slurry was adjusted by ammonia water to the range of 9–10, then stirred in the atmospheric condition for 2 h. Next, the precipitate was introduced to 100 ml hydrothermal reactor and raised temperature to 433 K, and then maintained for 5 h. The precipitate was filtered, washed and then dried at 433 K for overnight. Dried catalyst was calcined at 823 K for 5 h, crushed and then meshed. Ru precursor (Ru(NO)(NO₃)₃, Alfa Aesar Co.) was dissolved in a de-ionized water and the Ru precursor solution was loaded on the calcined hydrotalcite-like material and calcined at 723 K for 5 h. In the case of Ca and Zn modified hydrotalcite-like catalyst, Ca and Zn nitrate solution was added before the addition of ammonium carbonate solution the molar ratio of (Ca or Zn)/Mg was fixed to 0.5/5.5. Other Ru-supported catalyst was also prepared by impregnation method. Amount of Ru loading on the support was fixed to 5 wt%. The Ru-supported catalyst was calcined at 723 K for 5 h.

2.2. Catalyst characterization

BET surface area of the catalysts was determined by N₂ adsorption at 77 K, using the multipoint BET analysis method, with Moonsorption system (Moonsorp-II, KIST, Korea). Prior to the measurements, the samples were pretreated in a vacuum condition at 573 K for overnight. X-ray Diffraction (XRD) patterns were obtained using a Shimadzu XRD-6000 diffractometer with Cu K α radiation. The Scherrer equation was used to calculate the metallic crystal size from the XRD patterns. CO pulse chemisorption, TPR and NH₃-TPD were carried out by Micromeritics AutoChem 2060 system to determine a metallic particle size, dispersion and reduction states of Ru and acidity of the catalysts. The physical and chemical properties of prepared catalysts are summarized in Table 1.

2.3. Catalytic hydrogenolysis of glycerol

The conversion of glycerol to propanediol was carried out in an autoclave reactor system (Parr. Co.) with a 250 ml stainless steel reactor and stirred speed of 200–400 rpm. Prior to the reaction, the

catalyst was reduced by H₂ atmospheric condition at 573 K for 2 h. The reaction was carried out under the following conditions: 453 K, initial H₂ pressure of 2.5 MPa, 20 wt% glycerol aqueous solution of 50 ml, reduced catalyst of 0.3 g and reaction time of 18 h. After being purged by Ar and followed H₂ for 2 h and filled by H₂ to 2.5 MPa at room temperature, then the reactor was heated to the desired temperature. H₂ pressure was increased to about 4 MPa and slightly decreased during the reaction. After the reaction, products were analyzed by two gas chromatographs to measure glycerol conversion and selectivity of each products and 1,2-PDO yields. The liquid products were analyzed by FID GC (Agilent 7680A) equipped with INNOWAXTM capillary column. The gas product was analyzed by TCD GC (Agilent 6890N) equipped with CARBOSHPERETM packed column. The definition of glycerol conversion, selectivity of products and yields of 1,2-PDO are as followed Eqs. (1)–(3):

glycerol conversion(%)

$$= \frac{\text{amount of glycerol mole converted}}{\text{total amount of glycerol mole in the reactor}} \times 100 \quad (1)$$

i selectivity(%)

$$= \frac{\text{amount of glycerol mole converted to } i}{\text{amount of glycerol mole converted}} \times 100 \quad (2)$$

1, 2-PDO yield(%)

$$= \frac{(\text{glycerol conversion}(\%)) \times (1, 2\text{-PDO selectivity}(\%))}{100} \quad (3)$$

where i: 1,2-PDO, ethylene glycol, acetol, methanol, etc.

3. Results and discussion

3.1. Catalyst characterization

The crystalline phases of the prepared catalysts before and after the reaction were investigated by X-ray diffraction. Fig. 1 shows the XRD patterns of Ru-supported hydrotalcite-like or Ca-Zn modified hydrotalcite-like catalysts before (a) and after (b) the reaction. This crystalline pattern before reaction showed various patterns. MgAl₂O₄, MgO and RuO₂ crystalline phase were mainly found in Ru–Mg/Al catalyst. CaO, MgAl₂O₄ and RuO₂ showed in Ru–CaMg/Al catalyst. ZnO, MgAl₂O₄ and RuO₂ were found in Zn–Mg/Al and MgAl₂O₄ and RuO₂ phases were also found in Ru–CaZnMg/Al catalyst. It showed that hydrotalcite-based catalyst was changed to metal solid solution at 723 K and supported Ru was exposed on the catalyst during calcination. It was noted that the Layered Double Hydroxide (LDH; such as hydrotalcite) was found in the catalysts. This LDH structure was formed due to the intrinsic properties of hydrotalcite-like material called ‘memory effects’, recovered its hydrotalcite structure when the calcined catalyst contacts with

Table 1
The physical and chemical properties of prepared catalysts.

Catalyst	Ru loading (wt%)	BET S.A. (m ² /g)	RuO ₂ size (nm) ^a	Ru particle size (nm)	Ru metallic S.A. (m ² /g)	Ru dispersion (%)	Acidity (μmol NH ₃ /g)	
							Weak	Strong
Ru–Mg/Al	4.92	145.4	23	14.4	1.66	8.2	1.14	43.5
Ru–CaMg/Al	4.93	121.2	24	14.1	1.64	8.8	0.68	55.4
Ru–ZnMg/Al	4.88	92.4	20	15.2	1.68	7.9	0.75	62.3
Ru–CaZnMg/Al	4.90	129.4	23	13.7	1.75	9.6	3.41	113.7
Ru/γ-Al ₂ O ₃ ^b	5.01	165.3	33	38.5	0.67	2.2	14.49	1.71

^a Particle size of RuO₂ was estimated from XRD data.

^b Catalyst was prepared by impregnation method.

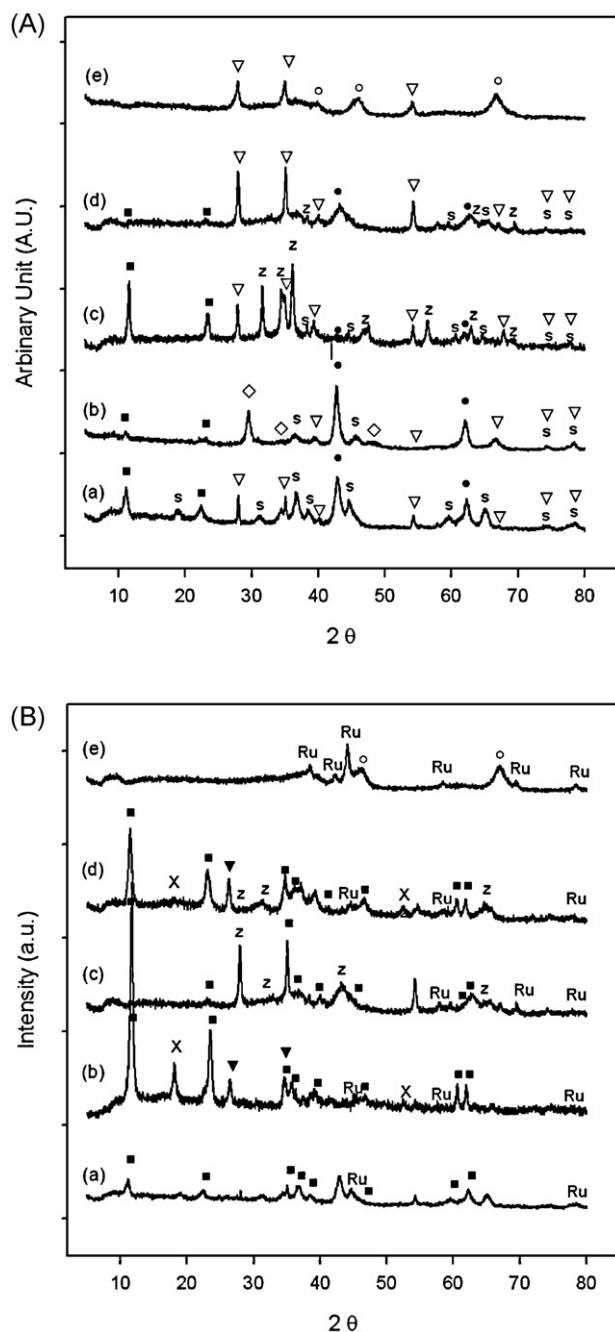


Fig. 1. XRD patterns of the prepared catalysts (A) before and (B) after the reaction: (a) Ru-Mg/Al, (b) Ru-CaMg/Al, (c) Ru-ZnMg/Al, (d) Ru-CaZnMg/Al and (e) Ru/ γ -Al₂O₃ (■: Hydrotalcite (Mg₄Al₂(OH)₁₂(CO₃)), ▽: RuO₂, □: CaO, ●: MgO, s: spinel (MgAl₂O₄), ○: γ -Al₂O₃, z: ZnO, X: Al₃Ca_{0.5}MgO₆).

moisture and carbonate ions [24]. The crystalline patterns of the hydrotalcite-like catalyst after the 1,2-PDO synthesis were different a lot. A LDH peak was mainly found in the used catalysts resulted from the 'memory effects' by contacting the catalyst on water during reaction. A little of Al₃Ca_{0.5}MgO₆ solid solution peak and ZnO peak were found in the used Ru-CaMg/Al, Zn-Mg/Al and Ru-CaZnMg/Al catalysts. XRD patterns of metallic Ru was found in the used catalysts but the Ru peak intensity was too low.

Fig. 2 shows TPR profiles of the prepared catalysts before PDO synthesis. All catalysts show one strong peak and shoulder peak at the temperature range of 450–525 K. The main peak corresponds to the reduction of RuO₂ to metallic Ru. It was reported that un-

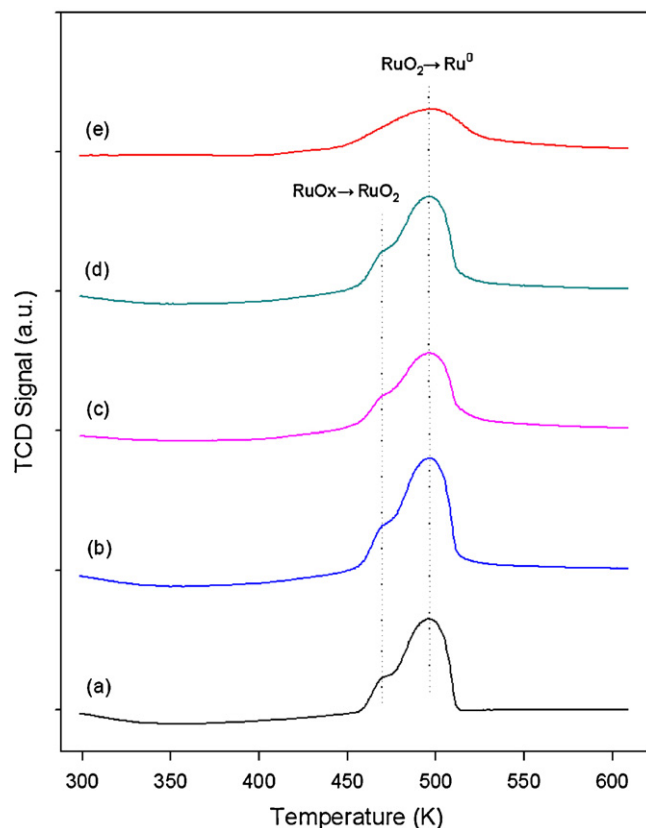


Fig. 2. TPR profiles of the prepared catalysts: (a) Ru/ γ -Al₂O₃, (b) Ru-Mg/Al, (c) Ru-CaMg/Al, (d) Ru-ZnMg/Al and (e) Ru-CaZnMg/Al.

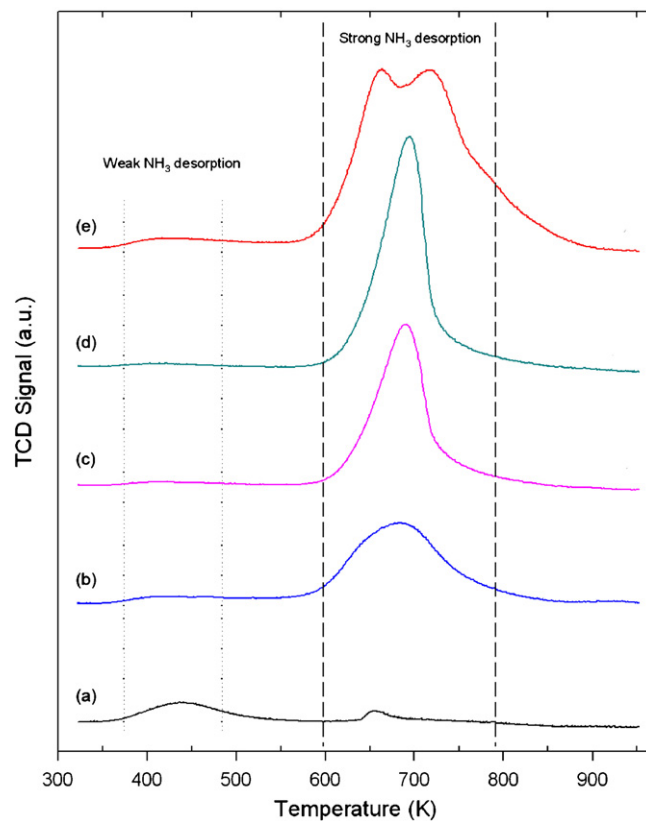


Fig. 3. NH₃-TPD profiles of the prepared catalyst: (a) Ru/ γ -Al₂O₃, (b) Ru-Mg/Al, (c) Ru-CaMg/Al, (d) Ru-ZnMg/Al and (e) Ru-CaZnMg/Al.

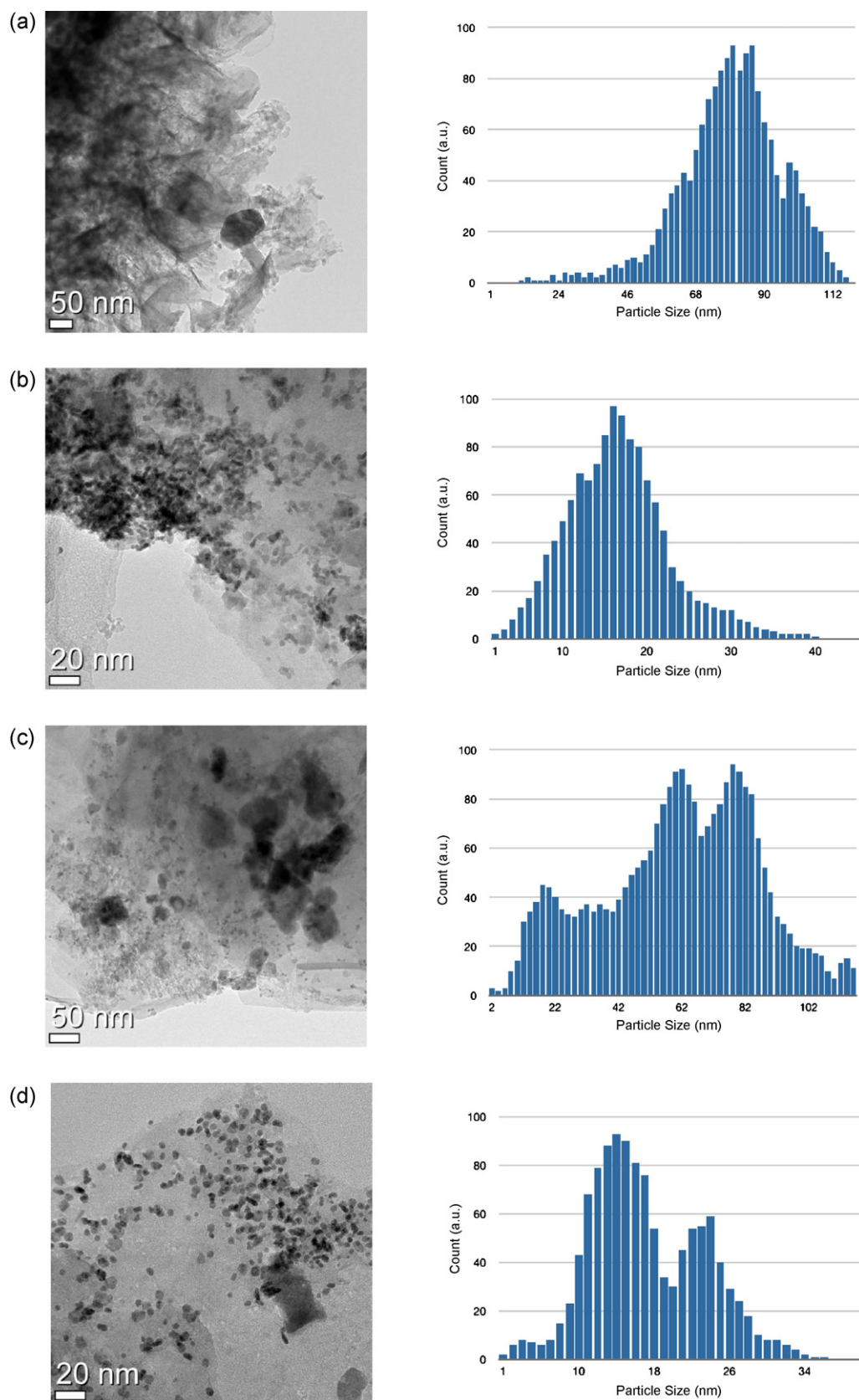


Fig. 4. TEM images and particle size distribution of the prepared catalysts: (a) Ru-Mg/Al, (b) Ru-CaMg/Al and (c) Ru-Zn/MgAl and (d) Ru-CaZnMg/Al.

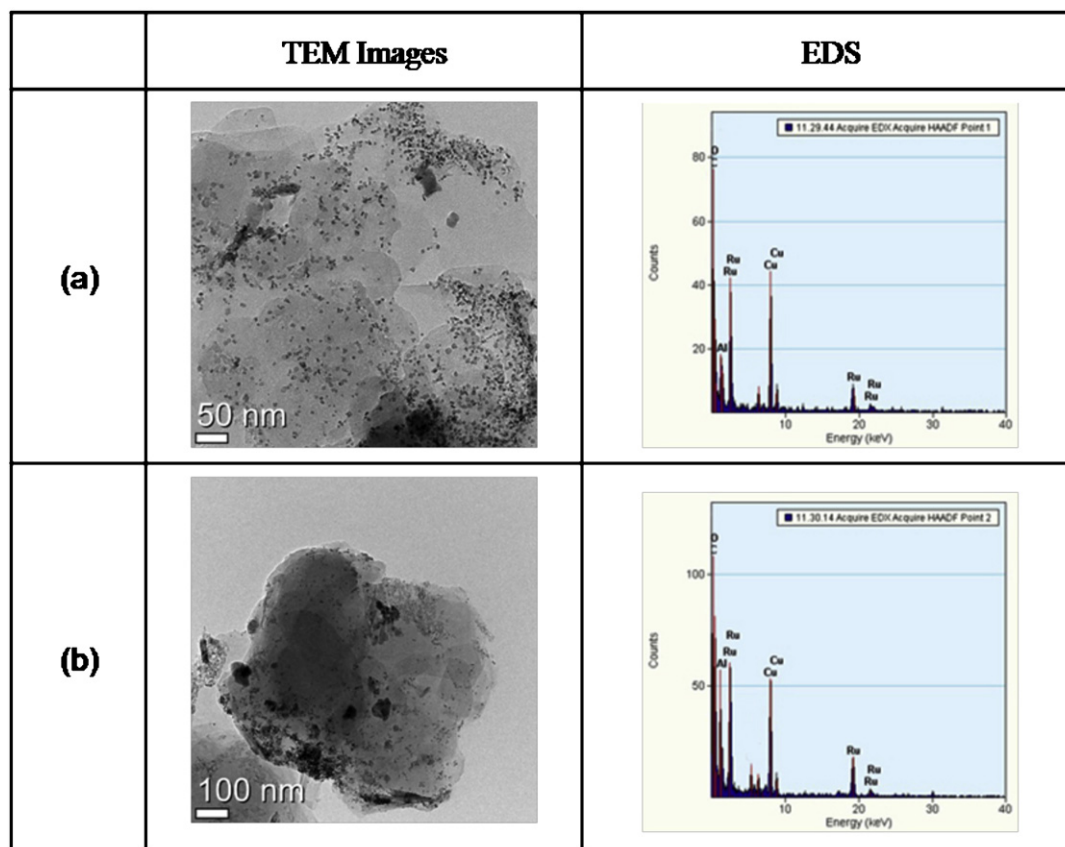


Fig. 5. EDS results on Ru–CaZnMg/Al catalysts (a) before and (b) after the reaction.

Table 2
Catalytic performance on glycerol hydrogenolysis over the prepared catalysts.**

Catalyst	Glycerol conversion (%)	Selectivity (%)					1,2-PDO yield (%)
		1,2-PDO	EG	2-PO	CH ₄	Other ^a	
Ru–Mg/Al	47.3	61.1	20.3	7.5	10.0	1.1	28.9
Ru–CaMg/Al	56.7	78.4	13.2	2.6	5.6	0.2	44.4
Ru–ZnMg/Al	55.6	75.1	14.9	3.8	5.9	0.3	41.8
Ru–CaZnMg/Al	58.5	85.5	6.6	1.9	5.6	0.4	50.0
Ru/γ-Al ₂ O ₃	45.6	59.2	22.3	5.4	11.1	0.2	27.0

** Reaction conditions: H₂ pressure of 2.5 MPa, 453 K of reaction temperature, catalyst of 0.3 g, 20 wt% glycerol solution of 50 ml, reaction time of 18 h and stirring rate of 200–400 rpm.

^a Sum of selectivities of acetol, 1,3-PDO, 1-PO (propanol), methanol, ethanol, CO and CO₂.

ported RuO₂ has been reported to reduce in a single main peak at 490 K [29]. It was considered that the main reduction peak is determined by the reduction of RuO₂ to Ru, and the shoulder peak has been related to the reduction of RuOx to RuO₂ [30,31]. However, it was found that the shoulder peak related to the reduction of RuOx

to RuO₂ was not investigated in the TPR profile of Ru–CaZnMg/Al catalyst. It was considered that the fraction of peak related to the reduction of RuOx to RuO₂ was less on this catalyst because the asymmetry of TPR peak over Ru–CaZnMg/Al catalyst was still observed.

Table 3
The effects of reaction temperature on selectivities in the hydrogenolysis of glycerol over Ru–CaZnMg/Al catalyst.**

Temperature (K)	Glycerol conversion (%)	Selectivity (%)						1,2-PDO yield (%)
		1,2-PDO	1,3-PDO	EG	2-PO	CH ₄	Other ^a	
393	28.5	45.3	15.4	10.6	10.3	8.2	10.2	12.9
413	37.7	58.1	5.3	9.5	7.4	9.3	10.4	21.9
433	51.3	71.8	1.5	8.7	4.2	9.7	4.1	36.8
453	57.8	85.4	–	6.6	0.8	5.6	1.6	49.4
473	61.9	70.3	–	17.4	–	11.5	0.8	43.5
493	63.1	61.5	–	23.7	–	14.3	0.5	38.8

** Reaction conditions: H₂ pressure of 2.5 MPa, 453 K of reaction temperature, catalyst of 0.3 g, 20 wt% glycerol solution of 50 ml, reaction time of 18 h and stirring rate of 200–400 rpm.

^a Sum of selectivities of acetol, 1-PO, methanol, ethanol, CO and CO₂.

Fig. 3 shows NH_3 -TPD profiles of the prepared catalysts. The acidity of the prepared catalysts is summarized in Table 1. The NH_3 -TPD profiles of Ru supported hydrotalcite-based catalysts showed a broad weak desorption peak in the temperature range of 380–450 K and strong desorption peak at 650–750 K. The high temperature peak indicates that strong acid site exists on the catalysts. It was noted that the Ru/ γ - Al_2O_3 catalyst showed the lowest acidity because Ru active species could be interacted and covered with the strong acid site on γ - Al_2O_3 more than hydrotalcite-based catalysts. It was found that the NH_3 -TPD profiles of Ru–CaZnMg/Al showed valley peak pattern range from 630 to 750 K, and more strong acid site distribution than the other catalysts. It was interpreted that the second peak (about 650 K) corresponded to NH_3 spillover of the catalyst and the third peak (about 740 K) associated with NH_3 decomposition on the active metal of the catalyst in higher temperature [32,33].

Fig. 4(a) exhibits the TEM images of Ru–Mg/Al catalyst. It was found that particle size of Ru–Mg/Al catalyst was mainly distributed in 50–100 nm and the small size of Ru particle less than 50 nm were not found in a particle size distribution data based on the TEM image. Fig. 4(b) shows the TEM images of Ru–Ca/MaAl catalyst. It was found that the particle size of Ru–CaMg/Al catalyst was smaller than Ru–Mg/Al catalyst and its particle size distribution was about 20–50 nm. It was considered that the smaller particle size of Ru was related to increase in glycerol conversion during hydrogenolysis. Fig. 4(c) shows the TEM images of Ru–ZnMg/Al catalyst. It was found that distribution of the particle size of Ru–ZnMg/Al catalyst was about 40–100 nm. A bit of the small Ru particles were showed on the surface of catalyst. Fig. 4(d) exhibits a TEM image of Ru–CaZnMg/Al catalyst. It was found that very small size of black-colored spherical-like shape particles about 5–10 nm were formed and exposed on the catalyst. It was found that the particle size of Ru was shifted to small size with the addition of Ca to Ru–Mg/Al.

Fig. 5 illustrates the EDS results before and after the reaction of the Ru–CaZnMg/Al catalyst. It was found that elements on black-colored spherical-like shape particles in the Ru–CaZnMg/Al catalyst was mostly Ru and some Mg and Al were detected. The results of TEM and EDS can be associated with Ru metallic particle size and dispersion by CO chemisorption as summarized in Table 1. Based on the results of particle size distribution and Ru particle size summarized in Table 1, it was considered that the smaller Ru particle on the catalyst acted as catalytic activity site during the hydrogenolysis of glycerol. It was found that the glycerol conversion and 1,2-PDO selectivity were increased with decreasing Ru metallic particle size and increasing Ru dispersion. It was considered that the particle size of the catalyst after the hydrogenolysis reaction was increased by the sintering of Ru particles.

3.2. Hydrogenolysis of glycerol

The hydrogenolysis of glycerol over the prepared catalysts was carried out at 453 K, initial H_2 pressure of 2.5 MPa, catalyst of 0.3 g, 20 wt% glycerol solution of 50 ml, stirred rate of 200–400 rpm for 18 h. The conversion of glycerol, selectivity of products and 1,2-PDO yield are summarized in Table 2. The results indicate that the prepared catalyst in this work shows high glycerol conversion over 45% and the main reaction product is 1,2-PDO in regardless of a type of support. However, selectivity of 1,2-PDO over Ru/ γ - Al_2O_3 catalyst was lower than the other catalyst. It was found that Ru–Mg/Al catalyst showed higher or nearly same glycerol conversion over Ru/ γ - Al_2O_3 , while selectivity and yield of 1,2-PDO were improved about 2% in the hydrogenolysis of glycerol. It was found that the glycerol conversion, 1,2-PDO selectivity and yield over Ca and Zn modified Ru-supported hydrotalcite-like catalyst (Ru–CaZnMg/Al) were higher than Ru–Mg/Al catalyst. The best catalytic performance over Ru–CaZnMg/Al catalyst was obtained with glycerol conversion

of 58.5%, 1,2-PDO selectivity of 85.5% and 1,2-PDO yield of 50.0%. Ru supported hydrotalcite-like catalyst showed higher Ru metallic surface area and dispersion than Ru/ γ - Al_2O_3 catalyst as shown in Table 1. With increasing Ru surface area and dispersion on the catalyst, the glycerol conversion was slightly increased. It was considered that the catalytic activity in glycerol hydrogenolysis was related to the dispersion of Ru.

Table 3 shows the effect of reaction temperature in the hydrogenolysis of glycerol over Ru–CaZnMg/Al catalyst. It was found that the glycerol conversion over Ru–CaZnMg/Al catalyst was increased with increasing the reaction temperature from 393 K to 493 K. The 1,2-PDO selectivity and yield were decreased when reaction temperature was more than 453 K.

The correlation between 1,2-PDO selectivity and acidity of the catalyst obtained by NH_3 -TPD analysis also exhibited in Table 2. It was found that 1,2-PDO selectivity was increased with increasing the acidity. LDH or hydrotalcite was known as weak base catalyst [23–25]. It was considered that catalyst acidity and 1,2-PDO selectivity was increased because small amount of Zn and Ca acted as Lewis acid site over the LDH or hydrotalcite in the glycerol dehydrogenation or carboxylation [2,34]. It was also found that the acidity of catalyst was drastically increased when both Ca and Zn were added at the same time which results in increasing glycerol conversion and 1,2-PDO selectivity.

4. Conclusions

The Ca and Zn modified Ru-based hydrotalcite-like catalyst prepared by solid phase crystallization and impregnation methods showed higher catalytic activity and 1,2-PDO selectivity than the other catalysts. The glycerol conversion and 1,2-PDO selectivity were obtained about 50% and 85%, respectively. Ru supported hydrotalcite-based catalysts were showed higher acidity and Ru dispersion than Ru/ γ - Al_2O_3 catalyst. It was found that the glycerol conversion and selectivity of the 1,2-PDO in glycerol hydrogenolysis were mainly corresponded to Ru dispersion and the acidity of the catalyst. The results can be interpreted that the acidity of the catalyst plays an important role in improving 1,2-PDO selectivity and Ru dispersion might be associated with activity, respectively.

Acknowledgements

We appreciate the financial supports from the Ministry of Knowledge Economy of Republic of Korea, J&K Heaters Co., Dansuk Industry Co. and JC Chemicals Co.

References

- [1] F. Ma, M.A. Hanna, *Bioresour. Technol.* 70 (1999) 1–15.
- [2] C.-H. Zhou, J.N. Beltrami, Y.-X. Fan, G.Q. Liu, *Chem. Soc. Rev.* 37 (2008) 527–549.
- [3] D.J. Moon, S.-H. Lee, E. Hur, S.H. Cho, J.S. Jung, M.J. Park, Y.J. Lee, G.J. Han, M.S. Chae, B.H. Kim, *Korea Patent* (2010) 10-2010-0099510.
- [4] E. Hur, D.J. Moon, *Trans. Korean Hydrogen New Energy* 21 (2010) 493–499.
- [5] S.-H. Lee, J.S. Kang, M.J. Park, H.-M. Park, S.D. Lee, D.J. Moon, *Proceeding of 9th Novel Gas Conversion Symposium*, 2010, p. P164.
- [6] S.H. Cho, D.J. Moon, *Proceeding of 2nd ASCON-IEECE*, 2010, p. CA3.
- [7] B. Casale, A.M. Gomez, *US Patent* (1994) 5,276,181.
- [8] S. Ludwig, E. Manfred, *US Patent* (1997) 5,616,817.
- [9] C. Tessie, *US Patent* (1987) 4,642,394.
- [10] C. Montassiera, J.C. Ménézoa, J. Moukoloa, J. Najaa, L.C. Hoanga, J. Barbiera, J.P. Boitiauxb, *J. Mol. Catal.* 70 (1991) 65–84.
- [11] J. Chaminand, L. Djakovitch, P. Gallezot, P. Marion, C. Pinel, C. Rosier, *Green Chem.* 6 (2004) 359–361.
- [12] T. Jiang, Y. Zhou, L. Shuguang, H. Liu, B. Han, *Green Chem.* 11 (2009) 1000–1006.
- [13] J. Zhou, L. Guo, X. Guo, J. Mao, S. Zhang, *Green Chem.* 12 (2010) 1835–1843.
- [14] M.A. Dasari, P.-P. Kiatsimkul, W.R. Sutterlin, G.J. Suppes, *Appl. Catal. A: Gen.* 281 (2005) 225–231.
- [15] L. Guo, J. Zhou, J. Mao, X. Guo, S. Zhang, *Appl. Catal. A: Gen.* 367 (2009) 93–98.

- [16] T. Miyazawa, Y. Kusunoki, K. Kunimori, K. Tomishige, *J. Catal.* 240 (2006) 213–221.
- [17] L. Ma, D. He, Z. Li, *Catal. Commun.* 9 (2008) 2489–2495.
- [18] M. Balaraju, V. Rekha, P.S.S. Prasad, B.L.A.P. Devi, R.B.N. Prasad, N. Lingaiah, *Appl. Catal. A: Gen.* 354 (2009) 82–87.
- [19] J. Feng, H. Fu, J. Wang, R. Li, H. Chen, X. Li, *Catal. Commun.* 9 (2008) 1458–1464.
- [20] E.S. Vasiliadou, E. Heracleous, I.A. Vasalos, A.A. Lemonidou, *Appl. Catal. B: Environ.* 92 (2009) 90–99.
- [21] D.J. Moon, S.D. Lee, S.-H. Lee, H.M. Park, G.J. Han, M.S. Chae, B.H. Kim, *Korea Patent* (2010) 10-2010-0035921.
- [22] J.G. Speight, *Lange's Handbook of Chemistry*, 6th ed., McGraw-Hill, New York, 1999, pp. 168–225.
- [23] F. Canani, F. Trifiro, A. Vaccari, *Catal. Today* 11 (1991) 173–301.
- [24] A. Vaccari, *Appl. Clay Sci.* 14 (1999) 161–198.
- [25] K. Takehira, T. Shishido, P. Wang, T. Takaki, *J. Catal.* 221 (2004) 43–54.
- [26] D.J. Moon, S.D. Lee, B.G. Lee, D.H. Kim, Y.J. Lee, K.P. Na, M.J. Kim, J.S. Choi, *Korea Patent* (2009) 10-2009-0009802.
- [27] D.H. Kim, J.S. Kang, Y.J. Leem, N.K. Park, Y.C. Kim, S.I. Hong, D.J. Moon, *Catal. Today* 136 (2008) 228–234.
- [28] D.J. Moon, *Catal. Surv. Asia* 12 (2008) 188–202.
- [29] P.G.J. Koopman, A.P.G. Kieboom, V.H. Bakkum, *React. Kinet. Catal. Lett.* 8 (1978) 389–393.
- [30] R. Lanza, S.G. Järås, P. Canu, *Appl. Catal. A: Gen.* 325 (2007) 57–67.
- [31] M.G. Cattania, F. Parmigiani, V. Ragaini, *Surf. Sci.* 211–212 (1989) 1097–1105.
- [32] W. Raróg-Pilecka, D. Szmigiel, Z. Kowalczyk, S. Jodzis, J. Zielinski, *J. Catal.* 218 (2003) 465–469.
- [33] M. Nagai, K. Koizumi, S. Omi, *Catal. Today* 35 (1997) 393–405.
- [34] M. Aresta, A. Dibenedetto, F. Nocito, C. Ferragina, *J. Catal.* 268 (2009) 106–114.